Journal of Photochemistry and Photobiology A: Chemistry 216 (2010) 1–7

Contents lists available at ScienceDirect

Journal of Photochemistry and Photobiology A: Chemistry

journal homepage: www.elsevier.com/locate/jphotochem

Aggregation of indoline dyes as sensitizers for ZnO solar cells

Yukako Sakuragi [a], Xiao-Feng Wang [a], Hidetoshi Miura [b], Masaki Matsui [a], Tsukasa Yoshida [a,*]

[a] Environmental and Renewable Energy Systems Division, Graduate School of Engineering, Gifu University, Yanagido 1-1, Gifu 501-1193, Japan
[b] Tsukuba Research Center, Chemicrea Inc., D-142-1-6, Sengen, Tsukuba, Ibaraki 305-0047, Japan

ARTICLE INFO

Article history:
Received 28 February 2010
Received in revised form 24 June 2010
Accepted 17 August 2010
Available online 8 September 2010

Keywords:
Dye-sensitized solar cells
ZnO
Indoline dye
Adsorption
Aggregation
Impedance

ABSTRACT

Properties of indoline dye, D149, as a sensitizer for electrodeposited porous ZnO has been studied in detail. Control of adsorption time and use of co-adsorbing cholic acid (CA) were essential to achieve high efficiencies, because of aggregation of D149 to worsen the fill factor of solar cells. Adsorption isotherm measured for D149 on ZnO powder indicated 1.5 layer adsorption at saturation. Use of CA significantly improved the cell performance as it prevents aggregation and decreases the amount of D149 adsorbed. Impedance analysis of the cells with different levels of dye loading showed that dye aggregates form deep traps to promote recombination even at low cell voltages, thus resulting in an *I–V* curve with rounded shoulder with poor fill factor. A new indoline dye DN-7 turned out to behave much better in this regard, allowing foolproof reproduction of stably high efficiencies as its aggregation is much more relaxed than D149 and worsening of the fill factor can be avoided.

1. Introduction

Dye-sensitized solar cells (DSSCs) are promising candidates of photovoltaic devices which can efficiently convert solar energy-to-electricity at substantially low cost [1,2]. The best DSSC is based on TiO_2 porous electrode prepared by sintering its nanoparticles at a high temperature (typically > 450 °C). In combination with poly-pyridine Ru (II) complexes, it has achieved high solar energy-to-electricity conversion efficiencies (η) up to 11% [3]. In order to reduce the production cost of DSSCs and also to achieve versatility in applications, use of plastic substrate is more preferable compared to glass substrate. However, it is difficult to reach the same high efficiencies in plastic solar cells, because high temperature annealing cannot be applied.

On the other hand, ZnO can often be processed at relatively low temperatures. It has similar band positions but higher carrier mobility than TiO_2 [4,5], and thus be an attractive alternative electrode material especially for realization of plastic DSSCs. We have developed a method to directly crystallize mesoporous ZnO thin films from water by use of organic dye molecules such as eosinY as a structure-directing agent (SDA) for cathodic electrodeposition of ZnO [6]. Because the entire process requires neither high temperature nor aggressive chemicals, soft electrode materials such as ITO coated PET films can be used as the substrate. Owing to its porous crystalline structure having both high crystallinity and high surface area, such ZnO thin films can perform as excellent photoelectrode material to achieve high collection efficiency of photogenerated charge carriers [7]. When it was combined with indoline dye, D149, having relatively wide absorption in the visible range, a high conversion efficiency of 5.6% could be achieved [6]. Achieving higher efficiency may become possible by finding a dye that sensitizes ZnO as efficient as D149 but absorbs in relatively wider wavelength region.

The above-mentioned success with the indoline dyes, however, was not readily achieved. Indoline dyes are often very sensitive to the conditions of their adsorption onto ZnO surface, such as the kind of solvent, temperature, dipping time and use of co-adsorbing chemicals. Even when the same dye molecule was used, its efficiency drastically changed depending on such conditions and optimization of them was a demanding work. By contrast, Ru complex on TiO_2 is relatively insensitive to the conditions of adsorption, probably because dye monolayer is spontaneously formed in this combination. It is therefore important to develop photosensitizer dye for ZnO not only to achieve high efficiency but also to facilitate the choice of adsorption conditions, in order to achieve high reproducibility of device performance, which should be essential for commercial production.

In this work, we have studied the influence of adsorption conditions on device performance taking D149 and cholic acid (Fig. 1) [8] as sensitizer dye and co-adsorbing agent, respectively, to be combined with electrodeposited porous ZnO electrode. Change of device performance was examined not only by *I–V* measurements but also by photocurrent action spectra and electrochemical impedance spectroscopy (EIS). Aside from such electrochemical

* Corresponding author. Tel.: +81 58 293 2593; fax: +81 58 293 2594.
E-mail address: tyoshida@gifu-u.ac.jp (T. Yoshida).

1010-6030/$ – see front matter © 2010 Elsevier B.V. All rights reserved.
doi:10.1016/j.jphotochem.2010.08.015

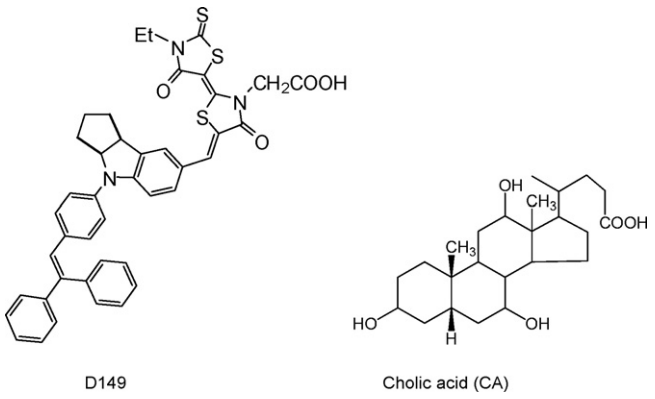

Fig. 1. Chemical structures of D149 and cholic acid molecules.

analysis, adsorption behavior of D149 was also studied. The origin of the changes of device performance and possibilities of its improvement are discussed.

2. Experimental

2.1. Electrodeposition of porous ZnO thin films

F-doped SnO_2 (FTO) coated glass (8 Ω/□, Asahi Glass) sheets were washed subsequently with detergent, acetone and 2-propanol. They were soaked in a 45% HNO_3 solution for 2 min and finally rinsed with water. They were used in a configuration of a rotating disk electrode (RDE) by attaching them to a commercial RDE system (Autolab) through a home-made attachment.

Electrodeposition of thin films was carried out in a single compartment cell equipped with an FTO glass RDE working, a Zn wire counter and a saturated calomel reference (SCE) electrodes. The temperature was kept at 70 °C by a thermostat in all experiments. A Hokuto-Denko HSV-100 voltammetric tool was used for potential control and current monitoring. The FTO glass working electrode was activated towards O_2 reduction by electrolysis at −1.2 V and 500 rpm rotation speed for 30 min in an O_2 saturated 0.1 M KCl (Merck) aqueous solution. Then, a small amount of concentrated $ZnCl_2$ (Merck) solution was added to the bath to achieve its concentration of 5 mM. A compact ZnO layer was electrodeposited at −1.1 V for 10 min. A stock solution of eosinY disodium salt (Kanto) was further added to the bath to be 50 μM in the bath and ZnO/eosinY hybrid thin film was electrodeposited at −1.0 V for 20 min. The resulting film was rinsed with water and soaked in a dilute KOH (Nacalai) aqueous solution (pH 10.5) for overnight to extract eosinY from the film. Such a procedure yielded thickness of compact layer and porous layer of ca. 1 and 3 μm, respectively.

2.2. Dye adsorption and cell fabrication

ZnO thin films were sensitized by soaking them in a 0.5 mM D149 solution in acetonitrile/tert-buthyl alcohol (v/v = 1/1) mixture, with or without 1.0 mM cholic acid (CA) at room temperature for controlled periods between 1 min and 25 h. The dyed ZnO electrode and a Pt-sputtered FTO glass counter electrode were assembled into a sandwich-type miniature (0.3 cm^2 area) cell using a hot-melt ionomer film as a spacer. Electrolyte solution consisting of 0.5 M tetrapropylammonium iodide (TPAI) and 0.05 M I_2 in acetonitrile/ethylene carbonate (v/v = 1/4) mixture was filled by capillary action. For EIS, the whole film in a round shape with 13 mm diameter was used to assemble a sealed cell with the electrode area of 1.13 cm^2 using a spacer film with a 12 mm round hole.

2.3. Photoelectrochemical measurements

I–V curves of the cells were measured by EKO MP-160 curve tracer under illumination with a simulated sun light (AM 1.5, 100 mW cm^{-2}) generated by a Yamashita-Denso YSS-150A. Photocurrent action spectra were measured on a Bunko-Keiki CEP-2000 system under monochromatic light illumination with a constant photon flux of 0.5×10^{16} s^{-1} cm^{-2}. A mask was applied to the cells to regulate the active area to 0.2 cm^2 in these measurements.

Ac impedance response of the cells were measured under illumination with a 200 W Xe lamp (Ushio) filtered for visible light and using a Solartron 1260/1287 system for a frequency range between 1 MHz and 10 mHz and for bias voltages between 300 and 700 mV.

2.4. Analysis of dye adsorption on ZnO

A known area of the dyed ZnO film was soaked in a measured volume of *N,N*-dimethylacetamide (DMA) for 24 h to desorb the dyes. Its UV–vis absorption spectrum was measured to determine the amount of adsorbed dye.

In order to measure adsorption isotherm, controlled amounts of ZnO nanoparticulate powder (TAYCA MZ-300, specific surface area = 30 m^2 g^{-1}) were added to 0.5 mM D149 solutions and stirred overnight at 40 °C to establish equilibria of dye adsorption. The ZnO particles were then separated by centrifugation (5000 rpm, for 10 min) and dye concentrations in supernatants were measured.

3. Results and discussion

3.1. Optimization of ZnO/D149 cells

Photovoltaic performance of a ZnO/D149 cell is highly sensitive to the soaking time of ZnO film in D149 solution for sensitization. Fig. 2 shows the change of the *I–V* curves of the cells under AM 1.5 light illumination (a) and in the dark (b). D149 is highly adsorptive to ZnO, so that the porous ZnO film could be nicely colored already after 1 min soaking. Consequently, the photocurrent reaches a relatively high value of close to 9 mA cm^{-2}. Extension of the soaking time to 10 min leads to an increase of photocurrent above 10 mA cm^{-2}. However, further increase of soaking time to 120 min results in a decrease of photocurrent.

These changes of photocurrent are nicely explained by the changes of the action spectra (Fig. 3). That of the cell with 1 min soaking time shows a relatively narrow and sharp peak at 540 nm with an incident photon to current conversion efficiency (IPCE) value of ca. 75%. For this sample, the light harvesting efficiency (LHE) is still limited due to small amount of adsorbed dye (see supporting information Fig. 1S for absorption spectra of D149 adsorbed ZnO thin films used in these measurements). IPCE is related to LHE together with the quantum efficiency of charge separation on photoexcitation of dye bound to ZnO (φ_{inj}) and the charge collection efficiency (η_{coll}) as follows:

$$\mathrm{IPCE} = \mathrm{LHE} \times \varphi_{inj} \times \eta_{coll} \quad (1)$$

so that LHE determines the shape of IPCE spectrum to reflect the absorption character of D149 molecule, when the LHE value is small. The IPCE of the sample with 10 min soaking time is higher for all wavelength than that with 1 min, due to the increase of LHE. While the highest value of about 85% is achieved around the absorption maximum, the effect of LHE increase is prominent especially for the wavelength range where light extinction coefficient of D149 becomes small, thus resulting in a significant broadening of the IPCE peak. The sample with 120 min soaking, on the other hand, shows a clear decrease of IPCE maximum down to about 70% accompanied

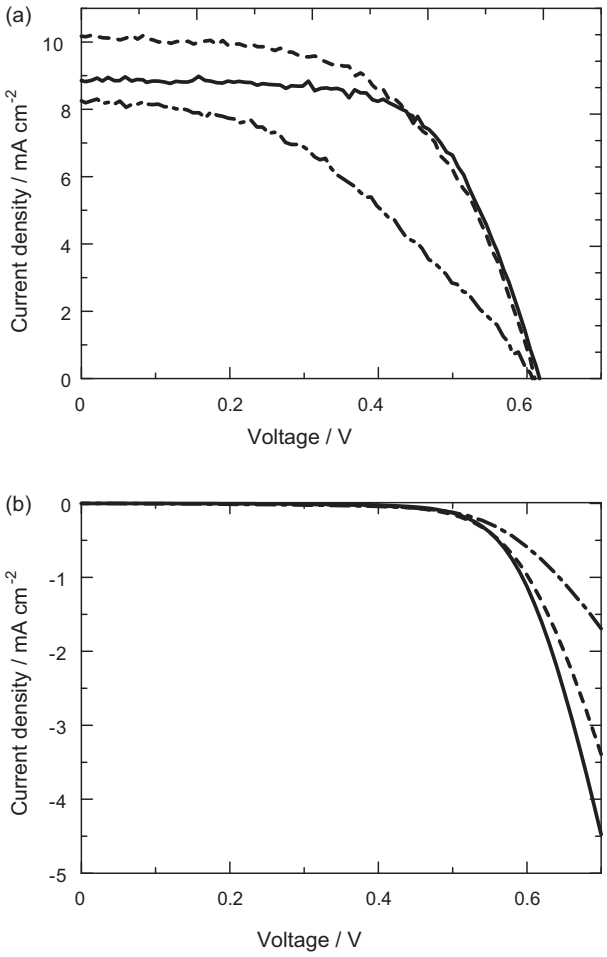

Fig. 2. *I–V* curves of the DSSCs employing electrodeposited porous ZnO thin films soaked in a D149 solution for 1 (—), 10 (- -), and 120 min (–·–) measured under illumination with an AM 1.5 simulated sun light (a) and in the dark (b).

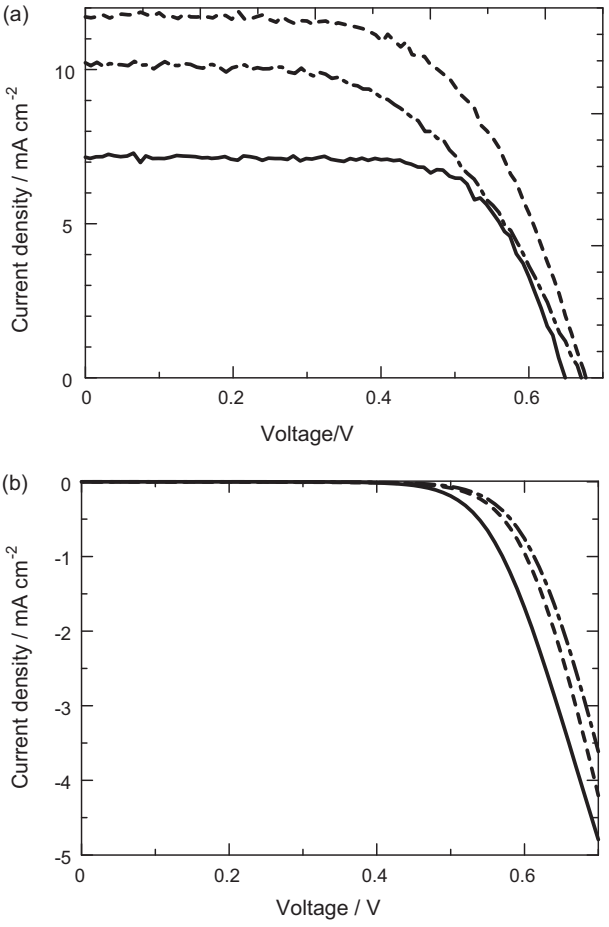

Fig. 4. *I–V* curves of the DSSCs employing electrodeposited porous ZnO thin films soaked in a mixed solution of D149 and cholic acid for 1 (—), 10 (- - -), and 120 min (–·–), measured under illumination with an AM 1.5 simulated sun light (a) and in the dark (b).

with a further broadening of the peak. For this sample, LHE is sufficiently high. Because η_{coll} is expected to be the same for all these cells as they employ the same electrode materials and electrolyte, the decrease of φ_{inj} should be responsible to the decrease of IPCE.

One can also notice from Fig. 2(a) significant worsening of the fill factor (*FF*) on extension of the soaking time as 0.64, 0.56 and 0.42 for 1, 10 and 120 min, respectively. When dark currents are compared (Fig. 2(b)), the extension of the soaking time causes a systematic decrease of the cathodic current that would indicate suppression of electron transfer from the electrode to I_3^- ions in the electrolyte owing to the better coverage of ZnO surface by D149 molecules. Open circuit voltage of the cells, however, almost stays constant, despite that the decrease of back reaction is usually believed to increase the electron concentration in the electrode, thus the increase of V_{oc} [9].

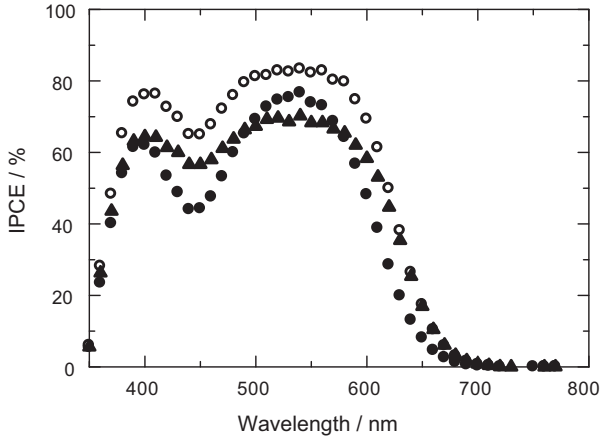

Fig. 3. Photocurrent action spectra of DSSCs employing electrodeposited porous ZnO thin films soaked in a D149 solution for 1 (●), 10 (○), and 120 min (▲).

These cell characteristics are significantly improved by co-adsorbing CA with D149. The *I–V* curves measured for the cells employing ZnO electrodes soaked in a mixture of D149 and CA are presented in Fig. 4. For the cell with 1 min soaking time, I_{sc} is much smaller than that without CA due to too small amount of D149, although a higher V_{oc} of ca. 650 mV is achieved. Also, *FF* of this cell is the highest (0.70). The highest current close to 12 mA cm^{-2} as well as the highest voltage of about 680 mV are achieved for the cell with 10 min soaking. The highest conversion efficiency of 4.78% was thus obtained under this condition as *FF* was only slightly worsened. However, extension to 120 min again resulted in a decrease of I_{sc} and worsening of *FF*, although the changes were more moderate than those without CA.

The changes of the cell performance were mainly associated with that of *FF* as one can see from the close correlation between *FF* and conversion efficiency (η) for different soaking time (Fig. 5). The *FF* of the cells continues to worsen on extension of the soaking time both with and without CA, although those with CA are always better than without. Without CA, the increase of I_{sc} by the increased

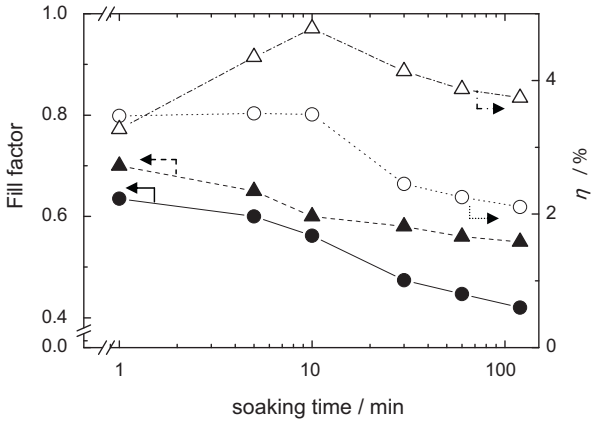

Fig. 5. Change of fill factor and conversion efficiency (η) of DSSCs on soaking time of ZnO film in solutions of D149 (circle) and D149 + CA (triangle).

amount of D149 is compensated by the worsening of *FF* to achieve constant η for the soaking time up to 10 min. The η then decreases by further worsening of *FF*. On the other hand, the cells with CA show an increase of η up to 10 min owing to the increase of I_{sc} and V_{oc} with moderately worsened *FF*. On further soaking, the η goes down due to the worsening of *FF*, although still much higher than those without CA.

3.2. Adsorption of D149 on ZnO

Even though a sort of optimum condition was found, the highly sensitive nature of D149 to the adsorption conditions is a serious problem when industrial mass production of solar cells is aimed. We have tried to identify the origin of this behavior. It appears that the extension of the soaking time leads to an overloading of D149 and then the worsening of *FF*. The amount of adsorbed D149 was therefore checked in the presence and absence of CA. D149 could be completely desorbed when the dyed film was soaked in dimethylacetamide (DMA). DMA is aprotic and a very good solvent of D149. In fact, no D149 can be adsorbed on ZnO when the film was soaked in a D149 solution in DMA. It is therefore obvious that D149 is simply adsorbed by ionic interaction and is not connected to ZnO surface through a chemical bond such as ester linkage as often spoken for DSCs [10].

The adsorbed D149 rapidly increases in the beginning of soaking and saturates after 60 min both with and without CA (Fig. 6). However, the saturation amount in the presence of CA is about 20% smaller than that without. It is confirmed that the amount of adsorbed D149 decreases by addition of CA because of its co-adsorption. Then, adsorption isotherm was measured in order to obtain further information about D149 adsorption on ZnO (Fig. 7). The low concentration half of the isotherm shows a quick rise and saturation of adsorption typical for a monolayer adsorption. However, it further increases when the concentration of dye in equilibrium goes higher than ca. 180 μM. Although the data points scatter quite a bit because the amount of ZnO powder added to dye solution for these data points were very small, the final saturation amount appears around 50% higher than that of the primary monolayer. The initial monolayer adsorption behavior could actually fit with Langmuir model that is expressed by

$$m = \frac{K_{ads} c M}{K_{ads} c + 1} \quad (2)$$

where m is the amount of adsorbed dye in equilibrium (in units of mol g^{-1} ZnO), M is the amount of adsorbed dye in saturation (mol g^{-1} ZnO), c is the concentration of dye solution in equilibrium, and K_{ads} is the adsorption stability constant in mol^{-1}. Data points up to c = ca. 150 μM reasonably fit with Eq. (2) and yielded K_{ads} = 64,300 mol^{-1} and $M = 8.26 \times 10^{-5}$ mol g^{-1} ZnO. Taking the nominal surface area of the ZnO powder that we used (30 m^2 g^{-1}), the area to be occupied by a single D149 molecule in the primary layer is calculated as 0.60 nm^2, that implies dye adsorption standing on the edge of the molecule, rather than being laid flat. The secondary layer appears as the half of the primary layer. One could therefore imagine that two adjacent D149 molecules in the primary layer provide a site for adsorption of another D149 molecule. About 20% reduction of the saturation amount in the presence of CA results from suppression of secondary layer formation due to co-adsorption of CA molecule in the primary layer. From these analyses, it has become clear that the change of *I–V* curve by soaking time and use of CA is related to the aggregation of D149.

3.3. Impedance analysis of ZnO/D149 cells

In order to clarify physical reasons for the worsening of *FF*, we have carried out electrochemical impedance spectroscopy (EIS) on the cells under the optimum conditions and that employing ZnO overloaded with D149. The equivalent circuit applied in the analysis of EIS response proposed by Bisquert [11,12] is presented in Fig. 8. The total resistance of the cell ($R_{tot}(U)$) which is the reciprocal of the slope (tangent line) of the *I–V* curve, thus is a function of the

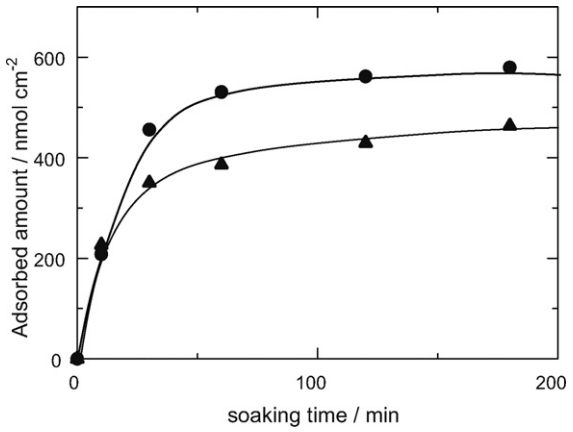

Fig. 6. Amount of adsorbed D149 measured for a 3 μm thick electrodeposited porous ZnO thin film soaked for controlled periods in solutions of D149 (circle) and D149 + CA (triangle).

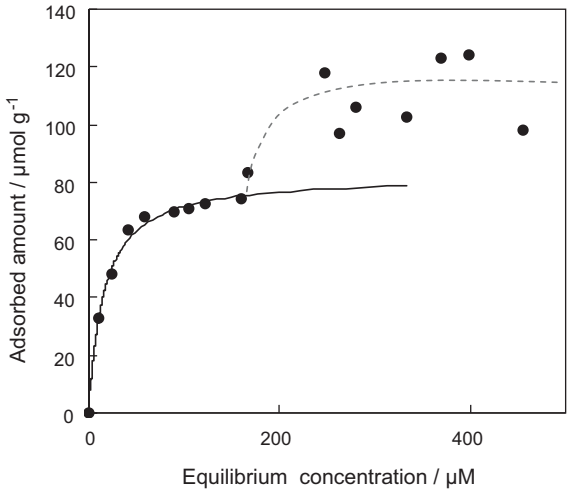

Fig. 7. Adsorption isotherm of D149 on nanocrystalline ZnO powder. The solid line indicates fitting according to Langmuir adsorption model, while the broken line indicates approximate trend of adsorption of the secondary layer.

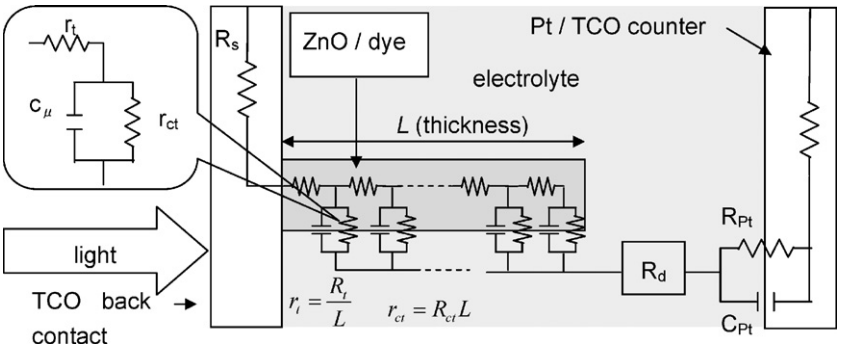

Fig. 8. Equivalent circuit used for the fitting of the EIS data measured in this study for the ZnO based DSSCs. See text for definition of each term.

cell voltage U, is the sum of the resistances at different interfaces as,

$$R_{tot}(U) = R_s + R_{Pt} + \frac{1}{3}R_t(U) + R_{ct}(U) + R_d \quad (3)$$

where R_s is the series resistance mainly imposed by the TCO glass substrate, R_{Pt} is the resistance of interfacial charge transfer at the counter electrode, $R_t(U)$ and $R_{ct}(U)$ are the charge transport and recombination resistances in the porous ZnO, respectively, both of which are expected to be dependent on the voltage thus the concentration of electron [13], and R_d is the Warburg resistance of ion transport in the electrolyte by diffusion.

Nyquist plots of EIS response measured at different cell voltages for a typical DSSC employing electrodeposited ZnO electrode are presented in Fig. 9. The plot close to the open circuit voltage gives three semicircles. The impedance on the real axis at the highest frequency end indicates R_s, while the three semicircles represent R_{Pt}, $1/3R_t(U)+R_{ct}(U)$ and R_d for the high, mid- and low frequency ranges, respectively, as indicated in the figure [14,15]. As the cell voltage becomes smaller, the semicircles become larger as expected for the increase of $R_{tot}(U)$. These plots at different U can be analyzed to determine each resistance and its dependence on the cell voltage is shown in Fig. 10 to be compared to the change of the I–V curve. As expected, the values of R_s, R_{Pt} and R_d are almost constant being independent on U, while the other two, $1/3R_t(U)$ and $R_{ct}(U)$, largely change by U. Increase of $1/3R_t(U)$ and $R_{ct}(U)$ on decrease of U is expected as the electron concentration in ZnO decreases [13]. The overall change of $R_{tot}(U)$ is mainly dominated by the change of $R_{ct}(U)$. The associated change of the I–V curve then can be divided into three regions: (I) $R_{tot}(U)$ is dominated by $R_{ct}(U)$ that is very large, thus I becomes nearly equal to I_{sc}, (II) $R_{tot}(U)$ changes by the change of $R_{ct}(U)$ thus changing I to create a curve and (III) $R_{tot}(U)$ becomes almost constant as dominated by R_s thus I changing linearly against U. The level of curvature of the I–V curve is therefore closely related to the change of $R_{ct}(U)$.

Since only $1/3R_t(U)$ and $R_{ct}(U)$ are dependent on U, these values are extracted from the EIS analysis on the cells with different levels of D149 loading (Fig. 11, See supporting information Fig. 2S for Nyquist plots of the EIS data and the I–V curves of the cells used for EIS). When $R_{ct}(U)$ of the cells are compared for U close to the open circuit voltage (ca. 600 mV and higher), adsorption of

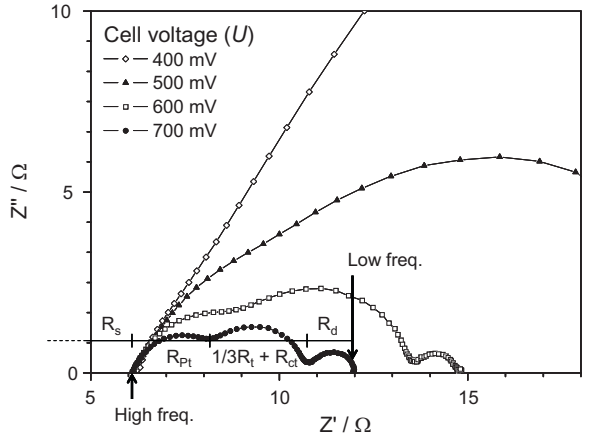

Fig. 9. Nyquist plots of EIS data measured at different cell voltages for a DSSC employing 3 μm thick electrodeposited ZnO sensitized with D149 (soaked for 10 min in a 0.5 mM D149 + 1 mM CA solution). Three semicircles correspond to different resistances as shown in the figure.

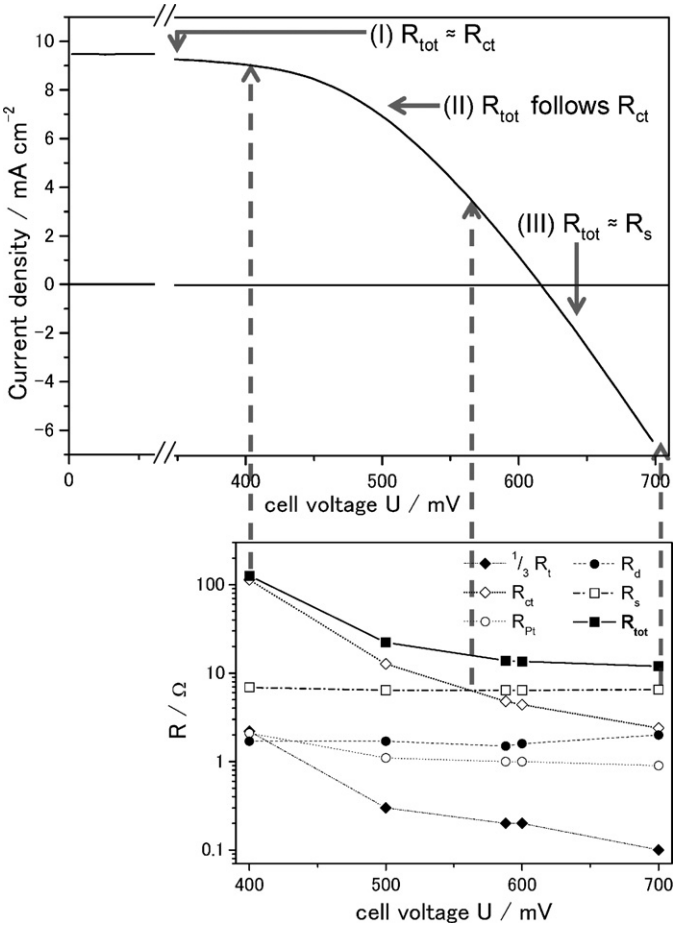

Fig. 10. I–V data measured at different cell voltages for a DSSC employing 7 μm thick electrodeposited ZnO sensitized with D149 (soaked for 1 h from 0.5 mM D149 + 1 mM CA solution).

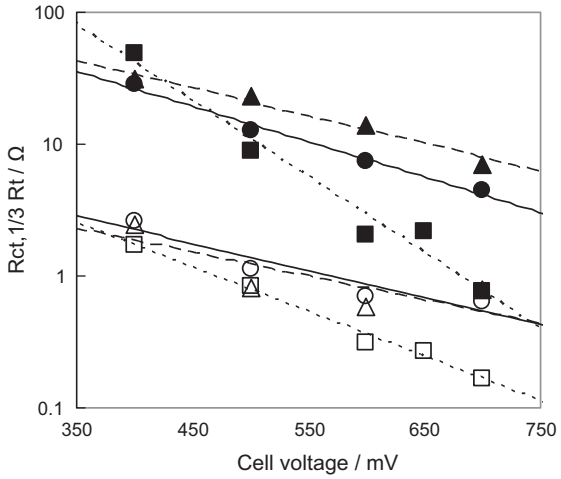

Fig. 11. $R_{ct}(U)$ (filled symbols) and the $1/3R_t(U)$ (open symbols) values determined by EIS measurements of DSSCs employing electrodeposited porous ZnO thin films soaked in solutions of D149 + CA for 1 h (square) and D149 for 5 (circle) and 25 (triangle) h.

D149 in a higher amount results in a higher resistance, in accordance with the decreased dark current in the *I–V* measurements (Figs. 2(b) and 4(b)). The better coverage of ZnO surface with D149 molecules leads to a less leaky surface. However, as the voltage thus electron concentration decreases, the $R_{ct}(U)$ of the overloaded cells remains low, while that of the optimum cell quickly increases to stop the back reaction, so that all of the photogenerated charges are collected at the back contact as the transport resistance $R_t(U)$ is much smaller. It is likely that aggregates of D149 create deep traps from which back electron transfer is catalyzed. As the electrons continue to leak even at small voltages, *I* of the overloaded cell remains smaller than I_{sc} in the wide range of *U* down to ca. 200 mV to end up with an *I–V* curve with rounded shoulder, i.e., poor *FF*. Even though the nature of the electron trapping at the dye aggregates is unclear, it has become evident that overloading of D149 results in a weakening of voltage dependence of $R_{ct}(U)$ to lose some of the photogenerated charges by recombination even at small cell voltages. Such pathways of back reaction could nicely be blocked by the use of CA and controlling soaking time to prevent dye aggregation. One can also find differences of $R_t(U)$ by the level of dye loading in Fig. 11. It appears that the surface concentration of dye molecule influences the transport of electron in the nanospaced ZnO. However, the transport resistance remains much smaller than all other resistances so that it cannot be the limiting factor in all cases. Also, discussion about the electron transport is beyond the scope of the present study.

3.4. New indoline dye DN-7 with suppressed aggregation

Searching for an optimum condition for D149 adsorption was experimentally possible. However, such a process is simply to find a "best compromise" and is not useful for industrial mass production of solar cells, because the performance of the cells will be poorly reproducible. Even though D149 is one of the best dyes for ZnO as it achieves high IPCE and η, it is unfortunately not the ideal partner for ZnO due to its tricky aggregation behavior.

We have synthesized various indoline dyes with different substituents and tested them as sensitizers for ZnO solar cells. Among them, we have found favorable characters from DN-7 shown in Fig. 12. The synthetic routes, 1H, and 13C NMR of DN-7 are provided in Supporting information (Fig. 4S). The only difference of DN-7 from D149 is the substituent on N atom of the indoline moiety, simply having a phenyl group, but caused a clear difference in the *I–V* curve with respect to the soaking time (Fig. 13). The hydrophobic interaction between adjacent DN-7 molecules are expected to be smaller than that of D149 having a bulky (2,2-diphenylethenyl)phenyl group, thus making DN-7 less aggregating than D149. Because of the same reason, DN-7 is less adsorptive than D149, so that appreciable amount of dye could be attached only after 10 min soaking time. On extension of the soaking time to 30 min, photocurrent increased due to the increased amount of dye and created a maximum efficiency of 4.38%. Further extension to 120 min, however, does not degrade the cell performance unlike D149. Photocurrent as well as *FF* stays almost constant.

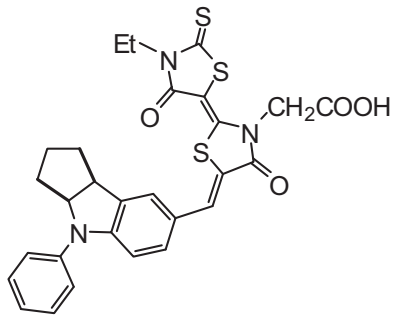

Fig. 12. Chemical structure of DN-7 dye.

Changes of *FF* and η against the soaking time are compared for D149 and DN-7 in Fig. 14. It is obvious that the worsening of *FF* in case of DN-7 is much more moderate than that of D149, although

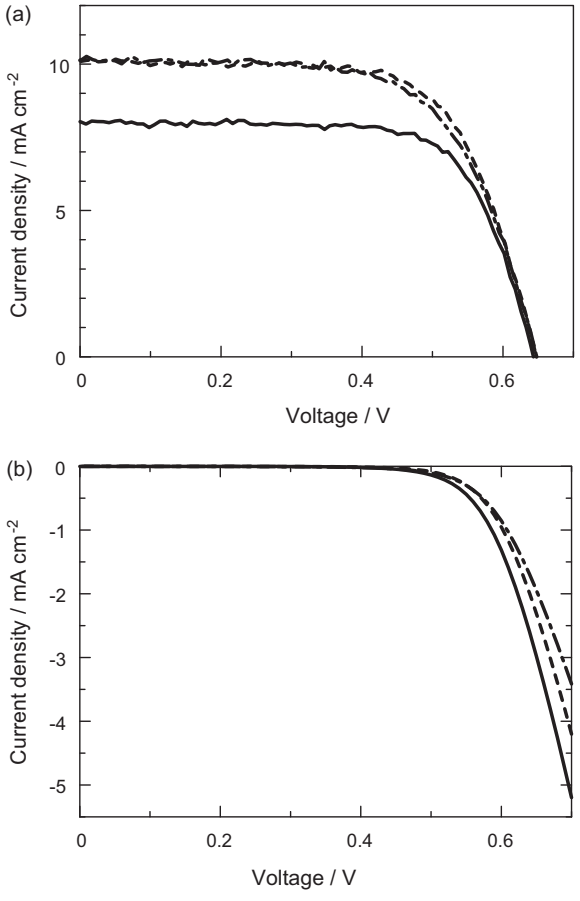

Fig. 13. *I–V* curves of the DSSCs employing electrodeposited porous ZnO thin films soaked in a mixed solution of 0.5 mM DN-7 and 1 mM cholic acid for 1 (—) 10 (- -), and 120 min (– –), measured under illumination with an AM 1.5 simulated sun light (a) and in the dark (b).

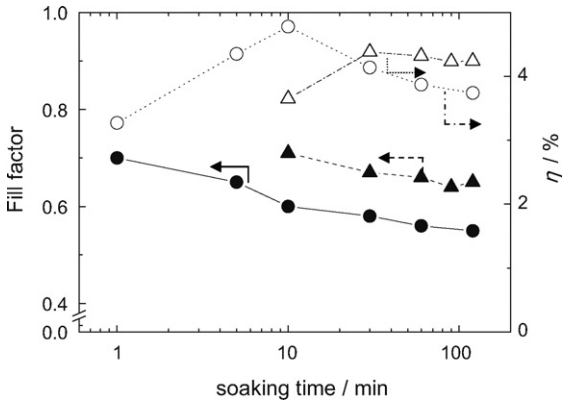

Fig. 14. Change of fill factor and conversion efficiency (η) of DSSCs on soaking time of ZnO film in solutions of D149 + CA (circle) and DN-7 + CA (triangle).

it does worsen slightly. Stably high efficiencies can be repeatedly achieved as DN-7 is less sensitive to the adsorption conditions than D149, and therefore is better suited to ZnO. Since the absorption band of DN-7 is slightly shorter than D149 (see supporting information Fig. 3S for absorption spectrum of DN-7), the maximum achievable current is smaller than that of D149 under the optimum conditions, thus the maximum η also being smaller. However, easy handling of DN-7 is its clear advantage, most likely caused by its less aggregating property. Dyes with such a chemical property and even broader absorption are therefore needed as the ideal partner for ZnO.

4. Conclusion

The reasons of difficulties for achieving high efficiencies using D149 as a sensitizer for ZnO solar cell have been clarified in the present study. Adsorption of D149 on ZnO does not stop as a monolayer, but results in aggregation in a higher order, most likely 1.5 layers as shown by the adsorption isotherm. EIS studies of the cells indicated that the aggregates serve as deep traps to make the electrode surface "leaky" against the back reaction even when the cell voltage becomes small, resulting in rounded *I–V* curves with poor fill factors. Such aggregation could only be suppressed by proper use of co-adsorbing species and controlling the level of adsorption less than that of the saturation. Highest efficiencies could only be obtained after such tuning of the process.

These problems of dye aggregation were relaxed very much with the new indoline dye DN-7. Even though the record efficiency of D149 (5.6% [6]) is still higher than that of DN-7, the choice of the sensitizer should not only be based on that. The foolproof character of DN-7 to achieve high efficiencies is beneficial not only for optimization of other parts of the devices such as nanostructure of ZnO and electrolyte composition but also for commercial production of them. In fact, we do not think that DN-7 is perfect as it is, because it still needs cholic acid to be co-adsorbed to prevent aggregation. The truly ideal dye should be such that it spontaneously forms a monolayer on ZnO without a help of co-adsorbing chemicals and stably achieve high efficiencies, combined with broad absorption for high current and suppression of recombination for high voltage.

Appendix A. Supplementary data

Supplementary data associated with this article can be found, in the online version, at doi:10.1016/j.jphotochem.2010.08.015.

References

[1] B. O'Regan, M. Grätzel, Nature 353 (1991) 737.
[2] M. Grätzel, Nature 414 (2001) 338.
[3] C.-Y. Chen, M. Wang, J.-Y. Li, N. Pootrakulchote, L. Alibabaei, C.-H. Ngoc-le, J.-D. Decoppet, J.-H. Tsai, C. Grätzel, C.-G. Wu, S.M. Zakeeruddin, M. Grätzel, ACS Nano 3 (2009) 3103.
[4] D.C. Look, Mater. Sci. Eng. B80 (2001) 383.
[5] E. Bellingeri, D. Marré, L. Pellegrino, I. Pallecchi, G. Canu, M. Vignolo, C. Bernini, A.S. Siri, Superlattices Microstruct. 38 (2005) 446.
[6] T. Yoshida, J. Zhang, D. Komatsu, S. Sawatani, H. Minoura, T. Pauporté, D. Lincot, T. Oekermann, D. Schlettwein, H. Tada, D. Wöhrle, K. Funabiki, M. Matsui, H. Miura, H. Yanagi, Adv. Func. Mater. 19 (2008) 17.
[7] T. Yoshida, M. Iwaya, H. Ando, T. Oekermann, K. Nonomura, D. Schlettwein, D. Wöhrle, H. Minoura, Chem. Commun. (2004) 400.
[8] M. Matsui, T. Fujita, Y. Kubota, K. Funabiki, H. Miura, M. Shiro, Bull. Chem. Soc. Jpn. 83 (2010) 709.
[9] H. Choi, S.O. Kang, J. Ko, G. Gao, H.S. Kang, M.-S. Kang, M.K. Nazeeruddin, M. Grätzel, Angew. Chem. Int. Ed. 48 (2009) 5938.
[10] X.-F. Wang, O. Kitao, E. Hosono, H. Zhou, S. Sasaki, H. Tamiaki, J. Photochem. Photobiol. A 10 (2010) 1016.
[11] J. Bisquert, G. G-Belmonte, F. F-Santiago, A. Compte, Electrochem. Commun. (1999) 429.
[12] J. Bisquert, Phys. Chem. Chem. Phys. 2 (2000) 4185.
[13] A.B.F. Martinson, M.S. Goés, F. F-Santiago, J. Bisquert, M.J. Pellin, J.T. Hupp, J. Phys. Chem. A 113 (2009) 4015.
[14] F. F-Santiago, E.M. Barea, J. Bisquert, G.K. Mor, K. Shankar, C.A. Grimes, J. Am. Chem. Soc. 130 (2008) 11312.
[15] F. F-Santiago, J. Bisquert, G. G-Belmonte, G. Boschloo, A. Hagfeldt, Sol. Energy Mater. Sol. Cells 87 (2005) 117.